

# BFACF-style algorithms for polygons in the body-centered and face-centered cubic lattices

E J Janse van Rensburg<sup>†§</sup> and A Rechnitzer<sup>‡</sup>

<sup>†</sup>Department of Mathematics and Statistics, York University  
Toronto, Ontario M3J 1P3, Canada

rensburg@yorku.ca

<sup>‡</sup>Department of Mathematics, The University of British Columbia  
Vancouver V6T 1Z2, British Columbia, Canada

andrewr@math.ubc.ca

**Abstract.** In this paper the elementary moves of the BFACF-algorithm [1, 2, 5] for lattice polygons are generalised to elementary moves of BFACF-style algorithms for lattice polygons in the body-centred (BCC) and face-centred (FCC) cubic lattices. We prove that the ergodicity classes of these new elementary moves coincide with the knot types of unrooted polygons in the BCC and FCC lattices and so expand a similar result for the cubic lattice (see reference [16]). Implementations of these algorithms for knotted polygons using the GAS algorithm produce estimates of the minimal length of knotted polygons in the BCC and FCC lattices.

PACS numbers: 02.50.Ng, 02.70.Uu, 05.10.Ln, 36.20.Ey, 61.41.+e, 64.60.De, 89.75.Da

AMS classification scheme numbers: 82B41, 82B80

§ To whom correspondence should be addressed (rensburg@yorku.ca)

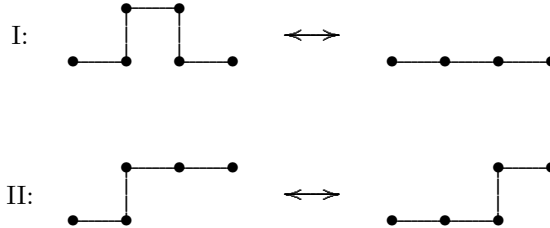


**Figure 1.** BFACF moves on a part of a square or simple cubic lattice polygon. Moves of type I are positive elementary moves when 2 edges are added, and negative elementary moves when 2 edges are removed. Moves of type II do not change the length of the polygon, and are called neutral elementary moves.

## 1. Introduction

The BFACF algorithm [1, 2, 5] is a Metropolis style Monte Carlo algorithm [17] that samples self-avoiding walks with fixed endpoints in the grand canonical ensemble in the hypercubic lattice  $\mathbb{Z}^d$ . The algorithm uses the local elementary moves in Figure 1 to sample walks along a Markov Chain from the (non-Boltzman) distribution

$$P_\beta = \frac{n e^{\beta n}}{\sum_{n \geq 0} n c_n(\mathbf{x}, \mathbf{y}) e^{\beta n}} \quad (1)$$

where  $\beta$  is a parameter and  $c_n(\mathbf{x}, \mathbf{y})$  is the total number of self-avoiding walks of length  $n$  from the lattice site  $\mathbf{x}$  to the lattice site  $\mathbf{y}$ .

The BFACF algorithm has also been used to sample unrooted polygons in the square and cubic lattices (see for example references [3, 4, 11, 12, 20, 21] and it has been generalised to lattice ribbons [19].

The BFACF algorithm can be used to sample knotted lattice polygons of fixed knot type [16] (also see [10] for a review) and has recently been used to determine the entropy and length of minimal knots in the cubic lattice [24, 25].

Despite its widespread use, the BFACF algorithm appears to have only been used in simple hypercubic lattices. In this paper our aim is to extend the elementary moves of the BFACF algorithm (see Figure 1) in the simple cubic lattice (hereafter referred to as the SC) to the body-centred and face-centred cubic lattices (hereafter referred to as the BCC and FCC lattices respectively). In addition, we examine the ergodicity properties of the proposed elementary moves when applied to unrooted self-avoiding polygons in the BCC and FCC lattices.

The BFACF algorithm is known to have elementary moves with non-trivial ergodicity properties in the cubic lattice [16, 8]. In this paper we prove an analogous result for the BCC and FCC lattices.

BFACF moves on walks or polygons (see Figure 1) have been generalised by re-interpretation as *plaquette atmospheres* (see [13]) — namely the ways in which edges can be added, deleted or shuffled around plaquette† adjacent to edges in the polygon. Examining the set of such possible moves has proved extremely useful (see [13]) and inspired generalisations of the Rosenbluth algorithm [23] to the GARM [22] and GAS algorithms [14, 15].

† Unit squares in the lattice bounded by four lattice edges

There are natural analogues of these plaquette atmospheres on the BCC and FCC lattices and the new elementary moves follow immediately from the definitions of these atmospheres; see Sections 3.1 and 4.1. While these moves are quite easy to define, some work is required to demonstrate their ergodicity properties.

In reference [15] an implementation of the BFACF elementary moves using the GAS algorithm was used to determine the shortest knots of given type in the simple cubic lattice. In this paper we extend those results by adding data for the BCC and FCC lattices, implementing the new BFACF-style elementary moves using the GAS algorithm. The minimal lengths of a selection of knot types in these lattices are displayed in Table 1. Knot types are indicated in the first column, while the next three columns give the lengths of the shortest knots of given type in each lattice. The last three columns are the number of distinct polygons (or “population”) of the lattice knots of minimal length.

**Table 1.** Minimal Knots in Cubic Lattices

Knot	Minimal Length			Population		
	SC	BCC	FCC	SC	BCC	FCC
$0_1$	4	4	3	3	12	8
$3_1$	24	18	15	3328	1584	64
$4_1$	30	20	20	3648	12	2796
$5_1$	34	26	22	6672	14832	96
$5_2$	36	26	23	114912	4872	768
$6_1$	40	28	27	6144	72	19008
$6_2$	40	28	27	32832	8256	5040
$6_3$	40	30	28	35522	3312	102720
$3_1^+ \# 3_1^+$	40	30	26	30576	14520	960
$3_1^+ \# 3_1^-$	40	30	26	143904	24048	960

In Section 2 we review the ergodicity properties of the BFACF elementary moves in the simple cubic lattice. We recall that the irreducibility classes of these moves, when applied to unrooted simple cubic lattice polygons, are the knot types of the polygons as embeddings of the circle in  $\mathbb{R}^3$ . This result, in particular, implies that two unrooted cubic lattice polygons  $\omega_1$  and  $\omega_2$  are in the same knot type if and only if there is a sequence of (reversible) BFACF elementary moves which will take  $\omega_1$  to  $\omega_2$  [16]. We generalise this result to the BCC and the FCC lattices.

In Section 3 we define an analogous set of elementary moves for polygons in the BCC lattice. We examine the properties of these moves and prove that the projection of any (unrooted) BCC polygon can be subdivided by application of the BCC elementary moves. A corollary of this result is that polygons can be made contact free — roughly speaking the polygon can be “inflated” so that non-consecutive vertices do not lie close to each other. This result is then used to sweep the BCC polygon into a sublattice isomorphic to the simple cubic lattice. In this sublattice the BCC elementary moves reduce to the usual BFACF moves. This is sufficient to show that the BCC elementary moves are irreducible on the classes of unrooted BCC polygons of given knot type.

Polygons in the FCC lattice are examined in Section 4. In this lattice the analogous of the cubic lattice BFACF moves is a single reversible elementary move which increases or decreases the length of an FCC lattice polygon by one. The proof

proceeds similarly to the BCC case, albeit with more cases. Again we show that any FCC lattice polygon can be made contact free and be swept onto a sublattice isomorphic to the simple cubic lattice. The usual set of simple cubic lattice BFACF moves can be performed on the polygon (in this sublattice) by compositions of the FCC elementary move. Similarly, this is sufficient to show that the FCC elementary moves are irreducible on the classes of unrooted FCC polygons of given knot type.

In Section 5 we show how the elementary moves may be used in a BFACF-style algorithm. This implementation samples from the distribution of polygons similar to that in equation (1). In addition, we note that the elementary moves can be implemented using the Metropolis algorithm instead, or using GAS-style sampling. We conclude the paper with a few final comments.

## 2. Knotted Lattice Polygons

Let  $S$  be the circle; we consider an injective map  $f : S \rightarrow \mathbb{R}^3$ , to be an *embedding* of the circle in Euclidean three space (that is,  $f$  is an injection, and is a homeomorphism onto its image). A polygon in the simple cubic lattice (SC), or the BCC lattice, or the FCC lattice, is a piecewise linear embedding of  $S$  into  $\mathbb{R}^3$ . Any such embedding of  $S$  is a *knot*, and if the embedding is a lattice polygon, then the embedding is a *lattice knot*. In this way cubic lattice polygons are lattice knots.

Two oriented embeddings  $f$  and  $g$  are ambient isotopic if there is an orientation-preserving isotopy  $H : \mathbb{R}^3 \times I \rightarrow \mathbb{R}^3 \times I$  (where  $I = [0, 1]$ ) with  $H(y, t) \equiv (h_t(y), t)$  such that  $h_0$  is the identity ( $h_0 \circ f = f$ ) and the composition  $h_1 \circ f = g$ . In other words, two lattice polygons are ambient isotopic if there is a continuous deformation of  $\mathbb{R}^3$  which takes the embedding  $f$  of the first polygon onto the embedding  $g$  of the second polygon.

Two lattice polygons in any cubic lattice (ie the SC, BCC or FCC lattices) are said to be equivalent if they are ambient isotopic. These equivalence classes of oriented embeddings of the circle into the cubic lattices define the knot types of *lattice knots*, see for example references [9] for a reviews and definitions of lattice knots.

In this paper we prove that there exists piecewise linear realisations of orientation-preserving ambient isotopies between lattice knots of the same knot type in the BCC and FCC lattices. These isotopies can be constructed as sequences of local deformations of the lattice knots in terms of BFACF-style elementary moves. This is an extension of a similar result for polygons on the simple cubic lattice in [16]. In that result, the piecewise linear orientation-preserving isotopies are realised in steps using the elementary moves of the BFACF algorithm, illustrated in Figure 1. By constructing the isotopies in this way in reference [16] the following result is proven:

**Theorem 1 (Thm 3.11 from [16])** *The irreducibility classes of the BFACF algorithm, when applied to unrooted polygons [in the simple cubic lattice], are the knot types of the polygons as piecewise linear embeddings in  $\mathbb{R}^3$ .  $\diamond$*

This, in particular, follows by proving that for every pair of (oriented) polygons  $(\omega, \nu)$  of the same knot type, there exists a finite sequence of elementary moves of either type I or II in Figure 1, such that these moves change  $\omega$  into  $\nu$ . Each move is a local deformation of the polygon and the ambient space around it, and is itself an isotopy. The sequence of moves is a composition of these local isotopies, and is itself a realisation of an isotopy  $H : \mathbb{R}^3 \times I \rightarrow \mathbb{R}^3 \times I$  such that  $H(y, t) \equiv (h_t(y), t)$  where  $h_0$  is the identity and  $h_1\omega = \nu$ .

In other words, the equivalence classes of polygons induced by the simple cubic lattice BFACF elementary moves in Figure 1 coincides with the knot types of the polygons, proving that the irreducibility classes of the BFACF algorithm are the knot types of unrooted polygons in the simple cubic lattice. In this paper, we extend this result to the BCC and FCC lattices — these extensions are Theorems 6 and 10 below.

### 2.1. Lattice Knot Projections

The BCC and FCC lattices are generated by finite sets of basis vectors  $\{\mathbf{c}_i\}$  and  $\{\mathbf{e}_i\}$ . Once the origin  $O$  of the lattice is set, then *vertices* are defined by linear combinations  $\sum_i p_i \mathbf{c}_i$  and  $\sum_i p_i \mathbf{e}_i$  respectively in the BCC and FCC, where the  $p_i \in \mathbb{Z}$  are finite signed integers. Thus, in each case the vertices have integer Cartesian coordinates.

Two vertices  $\mathbf{u}$  and  $\mathbf{v}$  are adjacent if the difference  $\mathbf{u} - \mathbf{v}$  is a basis vector of the lattice. In this case an *edge*  $\mathbf{uv}$  is defined between the vertices. The vertices  $\mathbf{u}$  and  $\mathbf{v}$  are the *end-vertices* of the edge  $\mathbf{uv}$ . We consider a lattice to be the collection of all its vertices and edges. Two vertices are adjacent if they are the endpoints of the same edge. Two edges are adjacent (or incident on one another) if they share exactly one end-vertex.

A *lattice polygon* is defined as a sequence or list of  $n$  adjacent edges  $\langle \mathbf{u}_0 \mathbf{u}_1, \mathbf{u}_1 \mathbf{u}_2, \dots, \mathbf{u}_{n-1} \mathbf{u}_0 \rangle$ , such that all vertices  $\{\mathbf{u}_0, \mathbf{u}_1, \dots, \mathbf{u}_{n-1}\}$  are distinct.

The *length* of the polygon is the number of edges  $n$  it contains (but its geometric length will generally be different from this, since the edges do not necessarily have length equal to one).

The BCC lattice is Eulerian with girth 4, and all lattice polygons in it have even length. The FCC lattice is Eulerian of girth 3, and polygons of length longer or equal to 3 can be realised in this lattice.

A lattice edge  $\mathbf{u}_i \mathbf{u}_j$  in the BCC lattice is said to be parallel to the  $\mathbf{c}_i$  direction, or *in the  $\mathbf{c}_i$  direction* if  $\mathbf{u}_j - \mathbf{u}_i = \mathbf{c}_i$ . Similarly, one may define edges to be in the  $\mathbf{e}_i$  direction in the FCC lattice. When a lattice edge in the BCC is parallel to the  $\mathbf{c}_i$  direction (or to the  $\mathbf{e}_i$  direction in the FCC), then we shall frequently abuse our notation by denoting it by its direction  $\mathbf{c}_i$  (or by  $\mathbf{e}_i$ ).

A *line segment* in a lattice polygon is a maximal non-empty sequence of adjacent edges in the polygon of the form  $\mathbf{c}_i \mathbf{c}_i \dots \mathbf{c}_i$  (in the BCC lattice), or  $\mathbf{e}_i \mathbf{e}_i \dots \mathbf{e}_i$  (in the FCC lattice). We say that these line segments are in the  $\mathbf{c}_i$  or  $\mathbf{e}_i$  directions respectively.

In what follows, we shall work with the *projections* of lattice polygons  $\omega$  into geometric planes  $A$  along a direction  $\mathbf{u}$ . To define these projections, consider two independent (unit) vectors co-planar with  $A$ , and let  $\mathbf{z} = \mathbf{x} \times \mathbf{y}$  be a vector normal to  $A$ . A vector  $\mathbf{u}$  is *transverse* to  $A$  if  $\mathbf{u} \cdot \mathbf{z} \neq 0$ .

The three vectors  $\{\mathbf{x}, \mathbf{y}, \mathbf{u}\}$  is the basis of a (non-orthogonal) coordinate system  $S$  in  $\mathbb{R}^3$ . Points in the polygon  $\omega$  can be identified by their coordinates in  $S$ , for example,  $\omega$  is a piecewise linear curve parametrised by  $t$  and each point  $\omega(t)$  has coordinates  $(\mathbf{x}_t, \mathbf{y}_t, \mathbf{u}_t)$ .

The *projection* of  $\omega$  into  $A$  along  $\mathbf{u}$  is defined by the set of points  $(\mathbf{x}_t, \mathbf{y}_t)$  in  $A$  for all values of the parameter  $t$ .

A *multiple point* in the projection of  $\omega$  into  $A$  along  $\mathbf{u}$  is a point in the projection which is the image two or more distinct points in  $\omega$ . A multiple point is a *double point* if it is the image of exactly two points.

In the case of lattice polygons, projections of polygons will be subgraphs of the projection of the lattice into a plane normal to a given lattice axes. For example, the

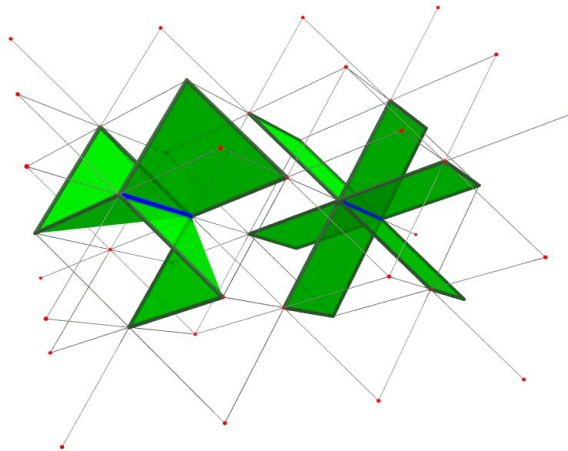


**Figure 2.** Nine of the 12 plaquettes adjacent to an edge in the BCC lattice. Note that the six on the right are planar, while the three on the left are non-planar. The remaining three (undisplayed) polygons are mirror-images of the three non-planar polygons.

projection of a simple cubic lattice polygon along the  $Z$ -direction into the  $XY$ -plane is a square lattice, and a cubic lattice polygon will project into a subgraph of this square lattice. This projection is a *lattice knot projection* in the square lattice; see reference [16].

In the BCC and FCC lattices we shall take projections of lattice polygons onto symmetry planes of the lattice, along directions which are transverse but not necessarily orthogonal to the symmetry planes.

### 3. BFACF-Style Elementary Moves in the BCC Lattice

In this section, we propose the local elementary moves of a BFACF-style algorithm in the BCC lattice and we show that they are sufficient to realise a piecewise linear orientation preserving isotopy on unrooted BCC polygons of the same knot type embedded in  $\mathbb{R}^3$ . In particular, this implies that the irreducibility classes of the BCC elementary moves coincide with the knot types of unrooted BCC polygons as determined by their embeddings in three space.

#### 3.1. BFACF style moves in the BCC lattice

In section 2.1 the notion of lattice polygons and projections of polygons were defined in general. We note in particular that the basis vectors of the BCC lattice are points in  $\mathbb{R}^3$  with Cartesian coordinates given by  $p\mathbf{c}_1 + q\mathbf{c}_2 + r\mathbf{c}_3 + s\mathbf{c}_4$  where  $p, q, r, s \in \mathbb{Z}$ , and where the vectors  $\mathbf{c}_i$  are given by

$$\begin{aligned} \mathbf{c}_1 &= (1, 1, 1), & \mathbf{c}_2 &= (1, 1, -1), & \mathbf{c}_3 &= (1, -1, 1), & \mathbf{c}_4 &= (1, -1, -1), \\ \mathbf{c}_5 &= (-1, -1, -1), & \mathbf{c}_6 &= (-1, -1, 1), & \mathbf{c}_7 &= (-1, 1, -1), & \mathbf{c}_8 &= (-1, 1, 1). \end{aligned}$$

Observe that  $\mathbf{c}_5 = -\mathbf{c}_1$ ,  $\mathbf{c}_6 = -\mathbf{c}_2$ ,  $\mathbf{c}_7 = -\mathbf{c}_3$  and  $\mathbf{c}_8 = -\mathbf{c}_4$ . The vectors  $\mathbf{c}_i$  the *generating* or *basis vectors* of the BCC and they all have (geometric) length  $\sqrt{3}$ .

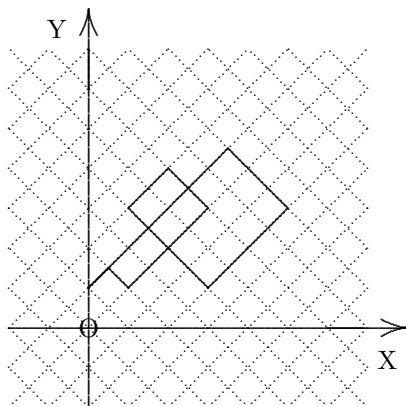


**Figure 3.** A projection of the BCC lattice and a BCC lattice polygon into the  $XY$ -plane. The projection of the BCC lattice is a square lattice rotated at  $45^\circ$  degrees with the Cartesian axes, and with edge-length  $\sqrt{2}$ . The polygon projects to a subgraph of the projected lattice.

Two vertices,  $\mathbf{u}$  and  $\mathbf{v}$ , are *adjacent* if they are separated by a single basis vector  $\mathbf{c}_i$ . Lattice edges will be in the  $\mathbf{c}_i$  directions in the BCC, and each lattice edge  $\mathbf{c}_i$  will be an edge in minimal length polygons of length 4 in the BCC lattice. These minimal length polygons containing  $\mathbf{c}_i$  bound 12 faces in the BCC, and these faces are not square and may not be planar in 6 of the cases. Nevertheless, we shall refer to them as lattice *plaquettes* – see Figure 2.

The (orthogonal) projection of the BCC lattice into the  $XY$ -plane is a geometric square lattice with edge lengths  $\sqrt{2}$  and rotated at  $45^\circ$  with respect to the  $X$ -axis. A polygon in the BCC projects to a subgraph of this square lattice. This is illustrated in Figure 3.

We define elementary moves on polygons in the BCC lattice by considering the 12 plaquettes adjacent to every edge  $\mathbf{c}_i$  (see Figure 2). Collectively, these plaquettes composed the *plaquette atmosphere* of the polygon [13]. In the simple cubic lattice, each edge is incident on at most 4 atmospheric plaquettes, and elementary moves of the BFACF algorithm are obtained by selecting an atmospheric plaquette and then exchanging edges along its boundary to update the polygon.

In particular, by taking the alternate path around the boundary of atmospheric plaquette BFACF moves in Figure 1 is obtained. A type I move on the simple cubic lattice performed by replacing a single edge incident on an atmospheric plaquette  $P$  in the polygon by the 3 edges in the alternative path around the boundary of  $P$ . This move is reversible, and together the move and its reverse defines type I moves. Similarly, a type II move on the cubic lattice replaces a pair of edges on incident on an atmospheric plaquette  $P$  with the other two edges in  $P$ .

The 12 atmospheric plaquettes incident on edges in BCC polygons will similarly be used to determine the set of elementary moves on BCC lattice polygons. A similar analysis to the above gives the following set of elementary moves on polygons in the BCC lattice:

#### BCC Elementary Moves:

- Replace an edge  $\mathbf{c}_1$  by  $\mathbf{c}_2\mathbf{c}_1\mathbf{c}_6$  (and all permutations of these vectors in the set of vectors  $\mathbf{c}_i$ ). This move increases the length of the polygon by 2. Conversely,

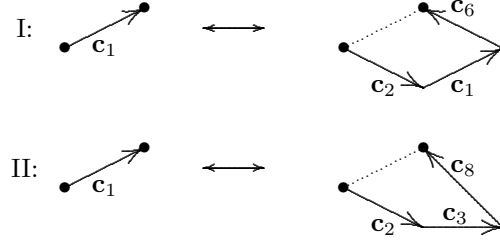


**Figure 4.** Replacing  $\mathbf{c}_1$  by three edges as shown defines an elementary move which increases the length of a polygon in the BCC lattice by two. This defines a *positive plaquette atmospheric move* on the polygon. Reversing the move gives a *negative plaquette atmospheric move* which reduces the length of the polygon by two edges by replacing three edges on the right by the single edge on the left. All the possible permutations of the vectors  $\mathbf{c}_i$  gives the complete collection of positive and negative plaquette atmospheric moves. Observe that closing the vectors on the right with the dotted line gives a square in case I, and a non-planar quadrilateral in case II.

replace  $\mathbf{c}_2\mathbf{c}_1\mathbf{c}_6$  by  $\mathbf{c}_1$  (and all permutations of these vectors) to obtain a move reducing the length of the polygon by 2. This move is illustrated (generically) by case I in Figure 4. Observe that the vectors  $\{\mathbf{c}_2, \mathbf{c}_1, \mathbf{c}_6\}$  are coplanar, so that  $\mathbf{c}_1\mathbf{c}_2\mathbf{c}_1\mathbf{c}_6$  forms a planar quadrilateral — a square. Hence, we call this the *planar BCC positive and negative plaquette atmospheric moves*, or the *planar BCC positive and negative elementary moves*.

- Replace an edge  $\mathbf{c}_1$  by  $\mathbf{c}_2\mathbf{c}_3\mathbf{c}_8$  (and all permutations of these vectors). This move increases the length of the polygon by 2. Conversely, replace  $\mathbf{c}_2\mathbf{c}_3\mathbf{c}_8$  by  $\mathbf{c}_1$  (and all permutations of these vectors) to obtain a move reducing the length of the polygon by 2. This move is illustrated by case II in Figure 4. Observe that the set of vectors  $\{\mathbf{c}_2, \mathbf{c}_3, \mathbf{c}_8\}$  is not coplanar; hence closing them off with  $\mathbf{c}_1$  bounds a non-planar quadrilateral or atmospheric plaquette. These are the *non-planar BCC positive and negative plaquette atmospheric moves*, or the *non-planar BCC positive and negative elementary moves*.
- Replace  $\mathbf{c}_1\mathbf{c}_6$  by  $\mathbf{c}_6\mathbf{c}_1$  (and all other permutations of these vectors). This is a neutral move, illustrated as case I in Figure 5. Note that these two pairs of edges form a square and so this move occurs in a plane in three space. These are the *planar BCC neutral plaquette atmospheric moves*, or the *planar BCC neutral elementary moves*.
- Replace  $\mathbf{c}_1\mathbf{c}_6$  by  $\mathbf{c}_3\mathbf{c}_2$  (all other permutations of these vectors). This is a neutral move, illustrated as case II in Figure 5. Now, these two pairs of edges form a non-planar quadrilateral or atmospheric plaquette and so this move does not occur in a plane in three space. More generally, these are the *non-planar BCC neutral plaquette atmospheric moves*, or the *non-planar BCC neutral elementary moves*.

Projecting the moves of Figures 4 and 5 into the  $XY$ -plane gives the (two dimensional) square lattice BFACF moves shown in Figure 1, but in the rotated square lattice of Figure 3 instead. Thus, by executing the BCC positive, negative and neutral plaquette atmospheric moves of Figures 4 and 5 on a polygon in the BCC, the image



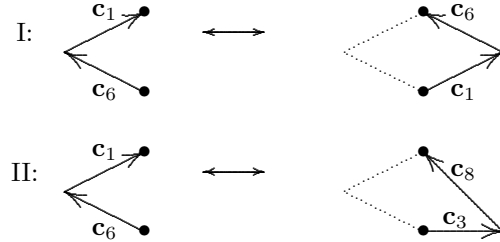


**Figure 5.** Replacing  $\mathbf{c}_6\mathbf{c}_1$  by either I:  $\mathbf{c}_1\mathbf{c}_6$  or by II:  $\mathbf{c}_3\mathbf{c}_8$  defines neutral plaquette atmospheric moves. Observe that  $\mathbf{c}_1 + \mathbf{c}_6 = \mathbf{c}_3 + \mathbf{c}_8$ . All the other possible neutral moves are obtained by using all the possible permutations of the  $\mathbf{c}_i$  in the above. Observe that by closing the vectors on the right into a quadrilateral along the dotted lines (which follows the path of  $\mathbf{c}_6\mathbf{c}_1$  between the bullets) gives a square in case I and a non-planar quadrilateral in case II.

of these moves in the projected square lattice include, as a subset, all the (usual simple square lattice) BFACF moves on the projected polygon.

### 3.2. Stretching polygons in the BCC lattice

We first outline our approach before we prove our main results. The proof of our main BCC lattice result in Theorem 6, is presented in two parts. We first show that any BCC lattice polygon can be swept onto a sublattice of the BCC which is isotopic to the simple cubic lattice (as an oriented embedded graph in three space). Then we show that in this sublattice we use the ergodicity properties of the simple cubic lattice BFACF algorithm [16] to complete the proof (see Theorem 1).

In other words, we shall show that any BCC lattice polygon can be swept into a sublattice  $\mathbb{L}$  with basis vectors  $\{\mathbf{c}_1, \mathbf{c}_3, \mathbf{c}_4, \mathbf{c}_5, \mathbf{c}_7, \mathbf{c}_8\}$ , and then show that a subset of the BCC elementary moves simulates a simple cubic lattice BFACF algorithm in this sublattice (which is not orthogonal but is nevertheless isotopic to the simple cubic lattice).

Our approach would be to demonstrate that the BCC elementary moves are sufficient to replace polygon edges outside the sublattice  $\mathbb{L}$  with edges in  $\mathbb{L}$ , while avoiding any self-intersections in the polygon as it is updated in this process. This is achieved by *stretching* the polygon to create sufficient space for executing BCC elementary moves (see Figure 6).

The stretching of a polygon will proceed by identifying a *maximal line* which intersect the projected polygon in its right-most and top-most projected edges. The polygon will be recursively stretched in directions normal to the maximal line by stretching parts of it across the maximal, while inserting edges to maintain its connectivity. We show that this can be done using the BCC elementary moves.

In particular, project the BCC lattice along the  $Z$ -direction onto the  $XY$ -plane, and let  $\omega$  be a BCC polygon with projection  $P\omega$  in the  $XY$ -plane. Then the image of the lattice and the polygon is the square lattice and a graph embedded in the square lattice illustrated in Figure 3. The *maximal* line  $K$  of  $P\omega$  is the line  $x + y = k$  with  $k$  the maximum value such that  $K$  has a non-empty intersection with  $P\omega$ .

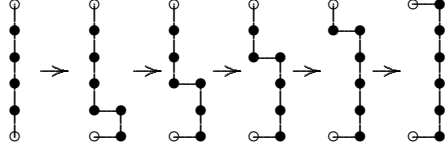


**Figure 6.** Translating a line segment with a single positive move and then a sequence of neutral moves in the BCC lattice, projected into the  $XY$ -plane. Since the projection of the polygon is to a square lattice, the BCC elementary moves project to square lattice BFACF elementary moves.

$K$  is the image of a plane  $P_r$  projecting parallel to the  $Z$ -axis into the  $XY$ -plane. We say that  $P_r$  is maximal if it intersects  $\omega$  and if it projects to the maximal line.

The maximal line  $K$  intersects the projection  $P\omega$  in projected line segments which lift to line segments and isolated vertices in  $\omega \cap P_r$ .

These definitions can now be used to stretch a polygon in a consistent way without creating self-intersections.

*3.2.1. Stretching a polygon in its maximal line:* Suppose  $L$  is a line given by  $x + y = l$  (with  $l \in \mathbb{N}$ ) which intersects the projected polygon  $P\omega$ . The maximal line  $K$  has equation  $x + y = k$ , and necessarily,  $k \geq l$ .

We say BCC basis vectors  $\mathbf{c}_i$  are *transverse* to the plane  $P_r$  if they are not parallel to  $P_r$ . Let  $\mathbf{c}_i$  be transverse to  $P_r$  — then  $\mathbf{c}_i \in \{\mathbf{c}_1, \mathbf{c}_2, \mathbf{c}_5, \mathbf{c}_6\}$ ; the other lattice vectors lie in  $P_r$ . Each line segment in this intersection can be translated one step in the  $\mathbf{c}_i$  direction by BCC elementary moves using the construction in Figure 6. We restrict such translations to be in the  $\mathbf{c}_i$  direction (with  $i = 1$  or  $i = 2$ ) in what follows. This will translate all line segments of non-zero length in the plane  $P_r$  in the  $\mathbf{c}_i$  direction.

This leaves the case of isolated vertices in  $P_r \cap \omega$ . The edges incident to and from these vertices will be of the form  $\mathbf{c}_1\mathbf{c}_6$  or  $\mathbf{c}_2\mathbf{c}_5$  (since  $K$  is maximal). In this case one may perform the move  $\mathbf{c}_1\mathbf{c}_6 \rightarrow \mathbf{c}_1\mathbf{c}_1\mathbf{c}_6\mathbf{c}_5$  or  $\mathbf{c}_2\mathbf{c}_5 \rightarrow \mathbf{c}_2\mathbf{c}_1\mathbf{c}_5\mathbf{c}_6$  to translate the isolated vertex in the  $\mathbf{c}_1$  direction. A similar construction will translate the segment in the  $\mathbf{c}_2$  direction instead.

Observe that no self-intersections can occur since all parts of the polygon in  $P_r \cap \omega$  are translated in parallel in the  $\mathbf{c}_i$  direction (with  $i = 1$  or  $i = 2$ ).

Once all line segments in the maximal plane  $P_r$  are translated in the  $\mathbf{c}_1$  (or  $\mathbf{c}_2$ ) direction, the polygon  $\omega$  is said to have been *stretched* in the plane  $P_r$  in the direction  $\mathbf{c}_1$ .

On completion of this construction, the maximal line  $K$  is translated to the line  $L$  by translating the plane  $P_r$  in the  $-\mathbf{c}_i$  direction. This plane is denoted by  $Q_r$  and is parallel to  $P_2$ . Then  $Q_r$  projects to  $L$  with formally  $x + y = \ell = k - 1$  in the  $XY$ -plane.  $L$  lifts to  $Q_r$ , and  $Q_r \cap \omega$  is a collection of line segments and isolated vertices of  $\omega$ .

Observe that the departing edges from  $Q_r$  to the maximal side arriving in  $P_r$  are all in the  $\mathbf{c}_i$  direction, since the polygon was stretched in that direction in the previous step.

In addition, the  $P_r$  contains no line segments, since these were translated into the  $\mathbf{c}_i$  direction. Furthermore, edges incident arriving in  $P_r$  from the opposite of the maximal side are parallel or anti-parallel to  $\mathbf{c}_j$  with  $j = 1$  or  $j = 2$ .

*3.2.2. Stretching a BCC polygon* We proceed by recursively executing the stretching of  $\omega$  in the  $\mathbf{c}_i$  direction in the plane  $Q_r$ . The intersection  $Q_r \cap \omega$  is a collection of line segments and isolated vertices in  $\omega$ .

If  $Q_r = P_r$ , where  $P_r$  projects to the maximal line  $K$ , then the situation is as described in the last section: We must consider two different cases in translating parts of the polygon in  $P_r$  in the  $\mathbf{c}_i$  direction. The first case involves line segments in  $P_r \cap \omega$ , the second case involves isolated vertices in  $P_r \cap \omega$ . Such a isolated vertices must have incident edges  $\mathbf{c}_1\mathbf{c}_6$  or  $\mathbf{c}_2\mathbf{c}_5$  (so as not to collide with  $P_r$ ). These two cases were already dealt with above.

In the event that  $Q_r \neq P_r$ , suppose that the stretching was recursively done starting in  $P_r$  and moving the plane in the  $-\mathbf{c}_i$  direction so that the last stretching was done in the  $\mathbf{c}_i$  direction in the plane  $Q'_r = Q_r + \mathbf{c}_i$ . Without loss of generality, one may suppose that the stretching is done in the  $i = 1$  direction. Then all edges between  $Q_r$  and  $Q'_r$  are parallel or anti-parallel to  $\mathbf{c}_1$ .

There are three different cases to consider. The first case involves line segments in  $Q_r \cap \omega$ , and the second case involves isolated vertices in  $Q_r \cap \omega$  with incident edges  $\mathbf{c}_1\mathbf{c}_6$  or  $\mathbf{c}_2\mathbf{c}_5$ . These two cases are done by translating the vertices and edges in the  $\mathbf{c}_1$  direction similarly to those line segments and isolated vertices in the plane  $P_r$  above: Since line segments projects to lines in the square lattice and BCC moves to BFACF moves in the square lattice, these line segments can be translated by applying BCC moves in the  $\mathbf{c}_1$  direction. Translating isolated vertices in the second case is similarly done.

The third and final case involves isolated vertices  $\mathbf{v}$  of the polygon in  $Q_r$  with edges on either side of  $Q_r$ . Suppose that these vertices are to be moved in the  $\mathbf{c}_1$  direction. Then the arrangements must be  $\mathbf{c}_1\mathbf{v}\mathbf{c}_1$ , or  $\mathbf{c}_2\mathbf{v}\mathbf{c}_1$ ; the middle vertex  $\mathbf{v}$  in these cases lies in  $Q_r$ , and the second edge moves from  $Q_r$  to a plane  $Q'_r = Q_r + \mathbf{c}_1$ .

In the cases  $\mathbf{c}_1\mathbf{v}\mathbf{c}_1$  the edges are left unchanged, since the departing edges to  $Q'_r$  are already in the  $\mathbf{c}_1$  direction. The case  $\mathbf{c}_2\mathbf{v}\mathbf{c}_1$  is updated to  $\mathbf{c}_1\mathbf{w}\mathbf{c}_2$ , with  $\mathbf{w}$  in the plane  $Q'_r$ . Observe that  $\mathbf{w}$  is always not occupied in  $Q'_r$  before the move, because all arriving edges from  $Q_r$  to  $Q'_r$  are in the  $\mathbf{c}_1$  direction before the moves are done.

In each case, these constructions give a polygon with departing edges from  $Q_r$  to  $Q'_r$  in the  $\mathbf{c}_i$  direction. Observe that the relative orientation of edges are again maintained, and that the moves are possible without any self-intersections in  $\omega$ .

The implementation of the stretching is recursive. Start in the plane  $Q_r = P_r$  which projects to the maximal line, and stretch the polygon a number of times in the  $\mathbf{c}_i$  direction transverse to  $Q_r$ . Then define  $Q'_r = Q_r$  and  $Q_r \rightarrow Q_r - \mathbf{c}_i$  recursively. This will stretch the polygon any desired length in each plane  $Q_r$  intersecting parallel to  $P_r$  without creating an intersection in the polygon.

The effect of the construction is to cut  $\omega$  along a plane  $Q_r$  and to move the two parts of  $\omega$  on either side of the polygon any number of steps in the  $\mathbf{c}_i$  direction transverse to  $Q_r$  apart while inserting edges parallel or anti-parallel to  $\mathbf{c}_i$  to reconnect it into a single polygon.

Observe that the construction does not change the knot type of  $\omega$ , and that it is the realisation of an ambient isotopy on the complementary space of the polygon. We say that we have *stretched* the polygon  $\omega$  in the  $\mathbf{c}_i$  direction along the plane  $Q_r$ . This completes the construction.

Observe that a similar construction will enable one to stretch  $\omega$  in directions transverse to lattice planes in the *BCC* transverse to any of the basis vectors  $\mathbf{c}_i$  of the BCC. This follows by exchanging the lattice basis vectors, such that a rotation of

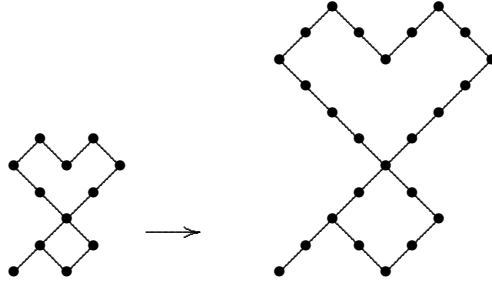


**Figure 7.** Stretching a projection of a BCC polygon. In this illustration, a polygon was stretched recursively in the projected directions until each projected edge was doubled.

the polygon preserving its chirality, is done in the above analysis. These observations complete the proof of the following theorem:

**Theorem 2** *Let  $\omega$  be an (unrooted) polygon in the BCC lattice with projection  $P\omega$  in the  $XY$ - $YZ$ - or  $XZ$ -plane. Let  $L$  be a line in the  $AB$ -plane with formula  $A \pm B = \ell$  where  $(A, B)$  is one of  $(X, Y)$ ,  $(Y, Z)$  or  $(X, Z)$ .*

*Suppose  $L$  intersects the projection  $P\omega$  and that  $\ell$  is an integer. Suppose also that  $L$  lifts to the plane  $Q_r$  parallel to the normal of the projection plane. Then  $\omega$  can be stretched along the plane  $Q_r$  in a direction  $\mathbf{c}_i$  transverse to  $Q_r$  by performing the BCC elementary moves in Figures 4 and 5 on  $\omega$ .  $\diamond$*

In Figure 7 we illustrate that a polygon can be recursively stretched until each projected edge has been replaced by two edges in the same projected direction. This is called the *subdivision* of the projected image of the polygon.

### 3.3. Contact free polygons

In this section we show that a given BCC polygon can be swept onto a sublattice  $\mathbb{L}$  with basis vectors  $\{\mathbf{c}_1, \mathbf{c}_3, \mathbf{c}_4, \mathbf{c}_5, \mathbf{c}_7, \mathbf{c}_8\}$ . This sublattice is isotopic to the simple cubic lattice, and once the polygon is contained in it, then a subset of the BCC moves reduces the usual BFACF moves.

In order to sweep a polygon  $\omega$  into  $\mathbb{L}$ , it is necessary to avoid self-intersections in the polygon when executing the necessary elementary moves. Such possible self-intersections are avoided by stretching the polygon, using the recursive subdivision explained in the previous section.

Two vertices  $\mathbf{v}$  and  $\mathbf{w}$ , non-adjacent in a polygon  $\omega$  (ie not connected by an edge in  $\omega$ ), form a *contact* if  $\mathbf{v} - \mathbf{w} = \mathbf{c}_j$  for some value of  $j$ .

Such a contact is said to be a *contact in the direction  $\mathbf{c}_j$* . A polygon  $\omega$  is *contact free* if it has no contacts. Observe that every contact is a lattice edge and projects to a line segment in the  $XY$ -plane. We show that by subdividing a polygon using the constructions outlined in the previous sections, one can make it contact free.

**Lemma 3** *By applying the BCC elementary moves in Figures 4 and 5 to an unrooted polygon in the BCC lattice, it can be transformed into a contact free polygon.*

*Proof:* Use BCC elementary moves to remove all contacts in the polygon  $\omega$  as follows.

If  $\omega$  has contacts in the  $\mathbf{c}_i$  direction, then subdivide the polygon such that the stretching is done in the  $\mathbf{c}_i$  direction. Since all edges in the  $\mathbf{c}_i$  direction will be doubled

up (effectively the scale of the polygons is changed such that every edge is replaced by two edges in a line segment of length 2), this removes all contacts in the  $\mathbf{c}_i$  direction. If there are still contacts in the  $\mathbf{c}_j$  direction (for some other  $j$ ), then subdivide the polygon in the  $\mathbf{c}_j$  direction.

Observe that if there no contacts in the  $\mathbf{c}_i$  direction, then stretching the polygon in the  $\mathbf{c}_j$  direction cannot create new contacts in the  $\mathbf{c}_i$  direction.

This follows because the creation of a contact in the  $\mathbf{c}_i$  direction will require the translation of parts of the polygon relative to one another in the  $\mathbf{c}_i$  direction, which does not occur when stretching in the  $\mathbf{c}_j$  direction.

Repeat the process of subdivision, until all contacts are removed and a contact free polygon is obtained.  $\diamond$

### 3.4. Pushing contact free BCC polygons into a simple cubic sublattice

Our goal is to show that every polygon in the BCC lattice can be changed into a polygon in sublattice  $\mathbb{L}$  which is isotopic to the simple cubic lattice by the applying the BCC elementary moves.

We defined  $\mathbb{L}$  to be that sublattice of the BCC with basis vectors  $\{\mathbf{c}_1, \mathbf{c}_3, \mathbf{c}_4, \mathbf{c}_5, \mathbf{c}_7, \mathbf{c}_8\}$ .  $\mathbb{L}$  is a non-orthogonal lattice, and if  $\omega$  is polygon in  $\mathbb{L}$ , then the subset of elementary moves in the BCC lattice which only involve the edges in the basis of  $\mathbb{L}$  reduces to the usual simple cubic lattice moves.

By lemma 3 one can show that BCC polygons can be made contact free and so we only have to examine contact free polygons in this section.

If  $\omega$  is a contact free polygon in the BCC, then it is pushed into  $\mathbb{L}$  by removing from it all edges in the  $\mathbf{c}_2$  or  $\mathbf{c}_6$  directions. The method of proof is as follows: Replace very edge in the  $\mathbf{c}_2$  direction by the three edges  $\mathbf{c}_1\mathbf{c}_4\mathbf{c}_7$  and every edge in the  $\mathbf{c}_6$  direction by three edges  $\mathbf{c}_5\mathbf{c}_8\mathbf{c}_3$ .

All that remains is to show that one can arrange matters such that self-intersections will not occur.

**Theorem 4** *By applying the classes of BCC elementary moves in Figures 4 and 5 to unrooted polygons in the BCC lattice, any such polygon can be swept into a polygon in the sublattice  $\mathbb{L}$ .*

*Proof:* Let  $\omega$  be a contact free polygon and subdivide it twice in each of the  $\mathbf{c}_1$ ,  $\mathbf{c}_5$ ,  $\mathbf{c}_3$  and  $\mathbf{c}_7$  directions. Then the shortest distance in the  $\mathbf{c}_1$  direction between vertices  $\mathbf{u}, \mathbf{v}$  not connected by an edge of the polygon is at least 3 steps. Similarly for the  $\mathbf{c}_5$ ,  $\mathbf{c}_3$  and  $\mathbf{c}_7$  directions.

We now show that edges in line segments in the  $\mathbf{c}_2$  or  $\mathbf{c}_6$  directions can be swept into the sublattice  $\mathbb{L}$ .

Replace edges in the  $\mathbf{c}_2$  or  $\mathbf{c}_6$  directions as follows:

- If  $\mathbf{c}_2\mathbf{c}_2\mathbf{c}_2 \dots \mathbf{c}_2$  is a sequence of consecutive edges in the  $\mathbf{c}_2$  direction, then replace them by  $\mathbf{c}_1\mathbf{c}_4\mathbf{c}_7\mathbf{c}_1\mathbf{c}_4\mathbf{c}_7 \dots \mathbf{c}_1\mathbf{c}_4\mathbf{c}_7$ .
- Similarly, replace any sequence of consecutive edges  $\mathbf{c}_6\mathbf{c}_6\mathbf{c}_6 \dots \mathbf{c}_6$  by the sequence  $\mathbf{c}_5\mathbf{c}_8\mathbf{c}_3\mathbf{c}_5\mathbf{c}_8\mathbf{c}_3 \dots \mathbf{c}_5\mathbf{c}_8\mathbf{c}_3$ .

These changes can be achieved by positive non-planar BCC elementary moves on the BCC polygon. Observe that these substitutions insert new vertices in the  $\mathbf{c}_1$ ,  $\mathbf{c}_5$  and  $\mathbf{c}_7$  and  $\mathbf{c}_3$  directions, adjacent to existing vertices in  $\omega$ , but that no contacts can be created since other vertices in these directions are a distance of at least three away.

The only intersections that can arise in the above construction do so at the endpoints of a sequence  $\mathbf{c}_2\mathbf{c}_2\mathbf{c}_2\dots\mathbf{c}_2$  or  $\mathbf{c}_6\mathbf{c}_6\mathbf{c}_6\dots\mathbf{c}_6$ . These are avoided as follows:

- If the edges at the beginning of the sequence  $\mathbf{c}_2\mathbf{c}_2\mathbf{c}_2\dots\mathbf{c}_2$  is  $\mathbf{c}_5\mathbf{c}_2\dots$ , then the substitution  $\mathbf{c}_2 \rightarrow \mathbf{c}_1\mathbf{c}_4\mathbf{c}_7$  on the first  $\mathbf{c}_2$  will cause an intersection (or a “spike”)  $\mathbf{c}_5\mathbf{c}_1\mathbf{c}_4\mathbf{c}_7\dots$ . If instead a neutral non-planar elementary move  $\mathbf{c}_5\mathbf{c}_2 \rightarrow \mathbf{c}_4\mathbf{c}_7$  is executed here, then the spike is avoided while the edge in the  $\mathbf{c}_2$  direction is removed.
- A similar argument holds if the sequence of  $\mathbf{c}_2$ 's ends as  $\dots\mathbf{c}_2\mathbf{c}_3$ , in which case one finds  $\mathbf{c}_2\mathbf{c}_3 \rightarrow \mathbf{c}_1\mathbf{c}_4$ .
- Similar arguments can be used to deal with the case of line segments of the form  $\mathbf{c}_6\mathbf{c}_6\dots\mathbf{c}_6$ .
- Lastly, if the line-segment has length one and is of the form  $\mathbf{c}_5\mathbf{c}_2\mathbf{c}_3$ , then one obtains the negative BCC elementary move  $\mathbf{c}_5\mathbf{c}_2\mathbf{c}_3 \rightarrow \mathbf{c}_5\mathbf{c}_1\mathbf{c}_4\mathbf{c}_7\mathbf{c}_3 \rightarrow \mathbf{c}_4$ .
- A similar argument holds for segments of the form  $\mathbf{c}_1\mathbf{c}_6\mathbf{c}_7$ .

Completion of these elementary moves produces a polygon with no edges in the  $\mathbf{c}_2$  or  $\mathbf{c}_6$  direction. This is exactly a polygon in the sublattice  $\mathbb{L}$ . This completes the proof.  $\diamond$

### 3.5. Irreducibility classes of the BCC elementary moves

By Theorem 4 all BCC lattice polygons can be changed into lattice polygons in the lattice  $\mathbb{L}$  which is isotopic to the simple cubic lattice. Since this process is reversible, one only has to consider polygons in  $\mathbb{L}$  and the effects of the BCC elementary moves on these polygons in this sublattice.

Restricting the BCC elementary moves to the sublattice  $\mathbb{L}$  implies that all elementary moves including either the directions  $\mathbf{c}_2$  or  $\mathbf{c}_6$  must be excluded. Observe that if both  $\mathbf{c}_2$  or  $\mathbf{c}_6$  are excluded from the set of BCC elementary moves (for example,  $\mathbf{c}_1 \leftrightarrow \mathbf{c}_2\mathbf{c}_1\mathbf{c}_6$  or  $\mathbf{c}_1 \leftrightarrow \mathbf{c}_2\mathbf{c}_3\mathbf{c}_8$ , are excluded) then the remaining moves reduce to the standard simple cubic lattice BFACF moves in Figure 1 in  $\mathbb{L}$ .

Thus if we restrict ourselves to this subset of possible moves on polygons in  $\mathbb{L}$  then we have the following lemma, which is a direct corollary of Theorem 1 or Theorem 3.11 in reference [16].

**Lemma 5** *The BCC elementary moves, restricted to the sublattice  $\mathbb{L}$ , applied to unrooted polygons in  $\mathbb{L}$ , have irreducibility classes which coincides with the knot types of the polygons as piecewise linear embeddings in  $\mathbb{R}^3$ .*  $\diamond$

Since every unrooted polygon in the BCC lattice can be (reversibly) reduced to a polygon in  $\mathbb{L}$ , the following theorem is an immediate corollary of Theorem 4 and the last lemma.

**Theorem 6** *The irreducibility classes of the BCC elementary moves, applied to unrooted polygons in the BCC lattice, coincides with the knot types of the polygons as piecewise linear embeddings in  $\mathbb{R}^3$ .*  $\diamond$

This completes the proof. In other words, it follows that the set of BCC elementary moves, applied to unrooted polygons in the BCC lattice, is irreducible within the knot type of the polygon.

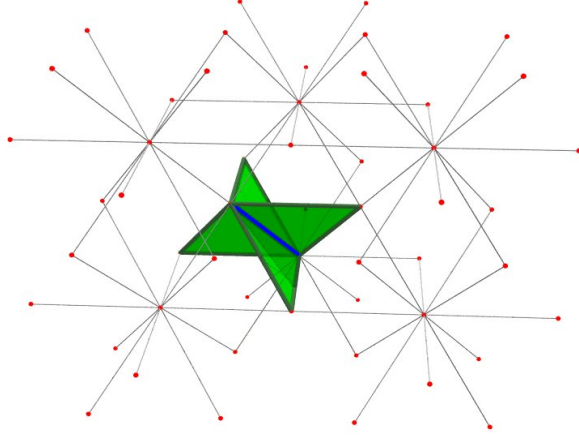


**Figure 8.** The four plaquettes adjacent to an edge in the FCC lattice.

#### 4. BFACF-Style Elementary Moves in the FCC Lattice

In this section we introduce local elementary moves of a BFACF-style algorithm on the FCC lattice; in fact there is only a single move that replaces two edges by a single edge and vice-versa. As was done for the BCC moves described above, we show that this new move is sufficient to realise a piecewise linear orientation preserving isotopy between two unrooted FCC polygons of the same knot type. This demonstrates that the irreducibility classes of the FCC elementary move coincide with the knot types of unrooted FCC polygons as determined by their embeddings in three space.

Local elementary moves in the FCC lattice have been explored previously in the literature, see for example references [7], however, the ergodicity properties of these elementary moves in the FCC have not been studied for knotted polygons.

##### 4.1. The FCC elementary move

Vertices of the face centered cubic (FCC) lattice are points in  $\mathbb{R}^3$  with positions given by the linear combinations  $p\mathbf{d}_1 + q\mathbf{d}_2 + r\mathbf{d}_3 + s\mathbf{d}_4 + t\mathbf{d}_5 + u\mathbf{d}_6$  where  $p, q, r, s, t, u \in \mathbb{Z}$ , and where the vectors  $\mathbf{d}_j$  is given

$$\begin{aligned}
 \mathbf{d}_1 &= (1, 1, 0), & \mathbf{d}_2 &= (1, -1, 0), & \mathbf{d}_3 &= (1, 0, 1), \\
 \mathbf{d}_4 &= (1, 0, -1), & \mathbf{d}_5 &= (0, 1, 1), & \mathbf{d}_6 &= (0, 1, -1), \\
 \mathbf{d}_7 &= (-1, -1, 0), & \mathbf{d}_8 &= (-1, 1, 0), & \mathbf{d}_9 &= (-1, 0, -1), \\
 \mathbf{d}_{10} &= (-1, 0, 1), & \mathbf{d}_{11} &= (0, -1, -1), & \mathbf{d}_{12} &= (0, -1, 1)
 \end{aligned}$$

We have labelled these vectors so that  $\mathbf{d}_{i+6} = -\mathbf{d}_i$ . We define *adjacent, lattice edges, end-vertices, lattice polygon* and *line segment* on the FCC lattice in the same way that we did on the BCC lattice. Note that a polygon of  $n$  edges on the FCC has geometric length  $n\sqrt{2}$ .

Observe that the sublattice generated by any set of three different non-coplanar vectors in the generating set of the FCC is isotopic to the simple cubic lattice. For example, the set  $\{\mathbf{d}_1, \mathbf{d}_3, \mathbf{d}_5\}$  generates a sublattice of the FCC which is isotopic to the cubic lattice (and may be viewed as a non-orthogonal simple cubic lattice).

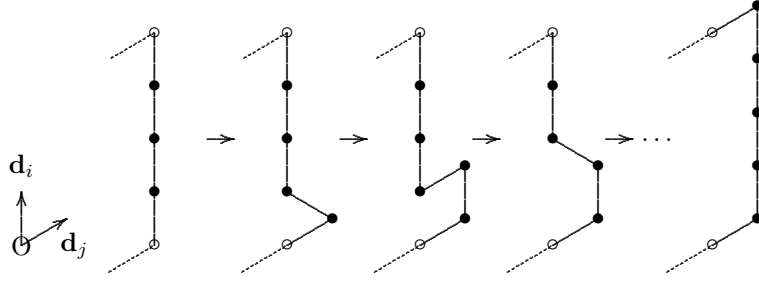


**Figure 9.** Translating a line segment in the  $\mathbf{d}_i$  direction in a polygon in the  $\mathbf{d}_j$  direction using the elementary move in the FCC lattice.

Similarly, there are sets of three coplanar vectors which generate a two-dimensional triangular lattice; for example, the set  $\{\mathbf{d}_1, \mathbf{d}_3, \mathbf{d}_{12}\}$  are the basis vectors of a triangular lattice in a plane with normal vector  $\mathbf{d}_1 \times \mathbf{d}_3$  (and observe that  $\mathbf{d}_{12} = \mathbf{d}_3 - \mathbf{d}_1$ ).

FCC Elementary Move:

- See Figure 8. Any vector  $\mathbf{d}_i$  in the FCC lattice is incident to four triangular plaquettes. That is, there are four different pairs of vectors  $(\mathbf{d}_j, \mathbf{d}_k)$  so that  $\mathbf{d}_i = \mathbf{d}_j + \mathbf{d}_k$ . The substitution of  $\mathbf{d}_i$  by  $\mathbf{d}_j \mathbf{d}_k$  is a *positive atmospheric FCC move*, or a *positive FCC elementary move* and it increases the length of the polygon by one edge. Similarly the reverse move, replacing  $\mathbf{d}_j \mathbf{d}_k$  by  $\mathbf{d}_i$  is a *negative atmospheric FCC move* or a *negative FCC elementary move* and it decreases the length of the polygon by one.

#### 4.2. Stretching polygons by using the FCC elementary move

In examining the irreducibility classes of the FCC elementary move, we shall follow the same strategy used for the BCC lattice in Section 3.

We first show that FCC polygons can be stretched, then made contact free, and finally swept into a simple cubic sublattice of the FCC. In this simple cubic sublattice of the FCC, the usual simple cubic lattice BFACF moves can be performed on the polygon by using combinations of the FCC elementary moves. Theorem 1 can then be used to complete the proof that the irreducibility classes of the elementary move coincides with the knot types of the polygon.

The basic construction in the proof is illustrated in Figure 9. By using the elementary move, the construction in Figure 9 shows that one can translate an entire line segment (in the  $\mathbf{d}_i$  direction one step in the  $\mathbf{d}_j$  direction, provided that  $\mathbf{d}_j \neq \pm \mathbf{d}_i$ ).

This construction can be performed regardless of the orientation of the edges incident at the ends of the line segments, provided that the set of target vertices in the  $\mathbf{d}_j$  direction are not occupied by the polygon.

Let  $\{\mathbf{d}_i, \mathbf{d}_j, \mathbf{d}_k\}$  be a triple which form a triangular plaquette in the FCC lattice (so  $\mathbf{d}_k = \mathbf{d}_j - \mathbf{d}_i$ ). Note that these three vectors generate a triangular sublattice  $T$  in the FCC; this sublattice is a geometric plane  $A$  with normal  $\mathbf{d}_i \times \mathbf{d}_j$ .

Consider the (non-orthogonal) projection of an FCC polygon  $\omega$  into the plane  $A$  along a lattice direction  $\mathbf{d}_l$  which is transverse to the plane  $A$  (that is,  $\mathbf{d}_l$  is not



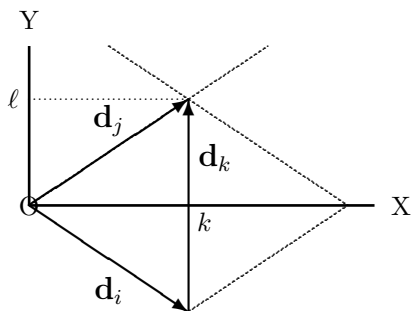


**Figure 10.** The vectors  $\{\mathbf{d}_i, \mathbf{d}_j, \mathbf{d}_k\}$  generate a triangular lattice in the plane  $A$ . The Cartesian coordinate system  $(X, Y)$  is set up with  $X$ -direction given by  $\mathbf{d}_i + \mathbf{d}_j$  and  $Y$ -direction given by  $\mathbf{d}_k$ . Observe that  $|\mathbf{d}_n| = \sqrt{2}$ , so that  $k = \sqrt{3}/2$  and  $\ell = 1/\sqrt{2}$ .

coplanar with vectors  $\{\mathbf{d}_i, \mathbf{d}_j, \mathbf{d}_k\}$ . We say that this projection is taken along  $\mathbf{d}_l$  into the  $\mathbf{d}_i\mathbf{d}_j$ -plane  $A$ .

In general, the projection of an FCC lattice polygon  $\omega$  along  $\mathbf{d}_l$  into the plane  $A$  is a lattice knot projection into a triangular lattice which is the projection of the FCC onto  $A$ . Define a two dimensional cartesian coordinate system in the plane  $A$  with  $Y$ -direction given by  $\mathbf{d}_k$  and  $X$ -direction by  $\mathbf{d}_i + \mathbf{d}_j$ . This is illustrated in Figure 10.

If  $P\omega$  is the projection of the polygon  $\omega$  in the plane  $A$  along a transverse lattice direction  $\mathbf{d}_l$ , then  $P\omega$  is a finite graph in the triangular lattice in  $A$ .

Hence, there exists a right-most line  $K$  parallel to the  $Y$ -axis (see Figure 10) which intersects the projection  $P\omega$ . We say that the line  $K$  is the *maximal* or *right-most* line *cutting* the projection  $P\omega$ . The right-most line is itself the projection of a plane  $P_r$  projected with  $\omega$  along the (non-orthogonal) direction  $\mathbf{d}_l$ . The intersection of this plane with the FCC lattice is a triangular sublattice of the FCC, generated by the set of basis vectors  $\{\mathbf{d}_k, \mathbf{d}_l\}$ .

Line segments in  $\omega$  are projected to line segments or to points in  $K$ , and these projected images lift back up to parts of the polygon in the intersection  $P_r \cap \omega$  of the plane and the polygon. Each line segment in this intersection can be translated one step in the  $\mathbf{d}_j$  (or  $\mathbf{d}_i$ ) direction (transverse to the plane  $P_r$ ) by using the basic constructions in Figure 9. If all the line segments in the plane which projects to the maximal or right-most line  $K$  are moved in the  $\mathbf{d}_j$  direction, then we say that the polygon is *stretched* in the  $\mathbf{d}_j$  direction from the plane  $P_r$ .

Observe that once a polygon has been stretched in the plane  $P_r$ , then there are no line segments in the polygon contained in  $P_r$ . This, in particular, implies that  $P_r \cap \omega$  is a collection of isolated vertices in  $\omega$ . At each such vertex  $\omega$  either passes through the plane to its right in the  $\mathbf{d}_j$  direction, or it turns to stay to the left of  $P_r$ . Projected images are illustrated in Figure 11.

Next we stretch the polygon in a plane  $P_r$  recursively starting in its right-most line  $K$ , and then successively moving left. Line segments in  $P_r \cap \omega$  can be moved in the  $\mathbf{d}_j$  direction using the construction in Figure 9. Since all the edges incident with  $P_r$  on the maximal side of  $P_r$  are in the  $\mathbf{d}_j$  direction, these constructions can be performed without creating any self-intersection.

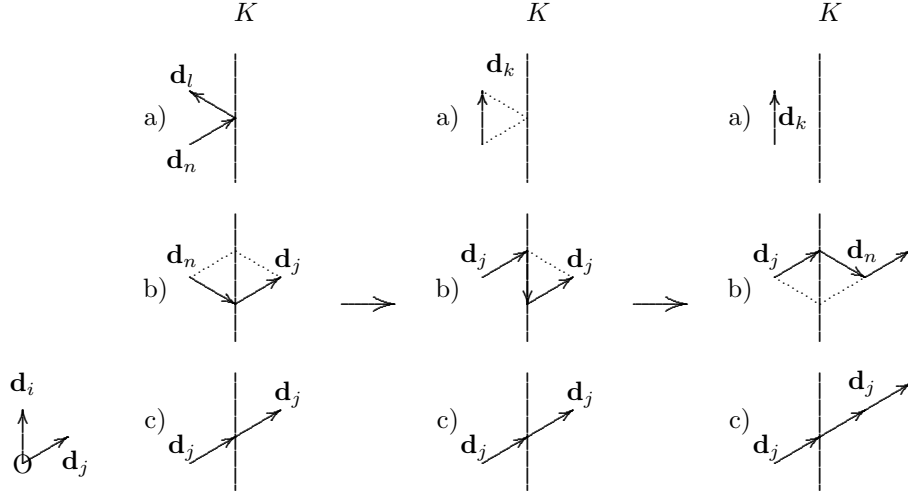


**Figure 11.** The projection of the polygon close to the maximal or right-most line  $K$  during the stretching of the polygon in the  $\mathbf{d}_j$  direction. The conformations of edges incident with the plane  $P_r$  are in general one of the cases above. In two cases the polygon passes through the  $P_r$ . In the third case it touches in one vertex before turning back. In this last case the vectors  $\mathbf{d}_n$  and  $\mathbf{d}_l$  must make an angle of  $60^\circ$  with one another. Cases as in (a) are removed as illustrated, while case (c) is left unchanged. In case (b) the edge in the  $\mathbf{d}_n$  direction is passed through the plane  $P_r$  in the direction  $\mathbf{d}_j$ . See Figure 12 for more details.

This leaves the cases of isolated vertices in  $P_r \cap \omega$ . The situation is as illustrated in Figure 11: All the parts of the polygon to the right of  $P_r$   $K$  been stretched in the  $\mathbf{d}_j$  direction, and the next step is to move parts of the polygon which has isolated vertices in  $P_r$  in the  $\mathbf{d}_j$  direction.

In Figure 11(a) we depict a situation in which the two vectors  $\mathbf{a}_n$  and  $\mathbf{a}_l$  must make a  $60^\circ$  angle with one another at the vertex in  $P_r$ . In this case we can remove these two edges from the polygon by making a negative atmospheric move replacing them with a single edge as shown. Thus we can eliminate this situation and we do not need to consider it in the discussion below.

Next, we address the situation depicted in Figure 11(b). We need to translate the edge  $\mathbf{d}_n$  in the  $\mathbf{d}_j$  direction. This is done as illustrated in Figure 12 (see also Figure 11). If the vertex marked by  $\circ$  in the left-most figure in Figure 12 is vacant (that is, not occupied by the polygon), then we can use two elementary moves to change the conformation  $\mathbf{d}_n\mathbf{d}_j$  to  $\mathbf{d}_j\mathbf{d}_n$ ; so the vector  $\mathbf{d}_n$  is translated in the  $\mathbf{d}_j$  direction, as desired.

On the other hand, if the vertex marked by  $\circ$  is occupied by another part of the polygon, then there are only two possibilities. First, it may correspond to the conformation depicted in Figure 11(a), in which case the elementary move can be used to remove the occupied vertex.

Otherwise it is the situation shown in the middle of Figure 12. In this case let  $Q$  be the plane coplanar with  $\{\mathbf{d}_j, \mathbf{d}_n\}$  and consider the line  $S = Q \cap P_r$ . Move along  $S$  in  $P_r$  until an open vertex  $\circ$  is encountered as shown the second and third parts of Figure 12.

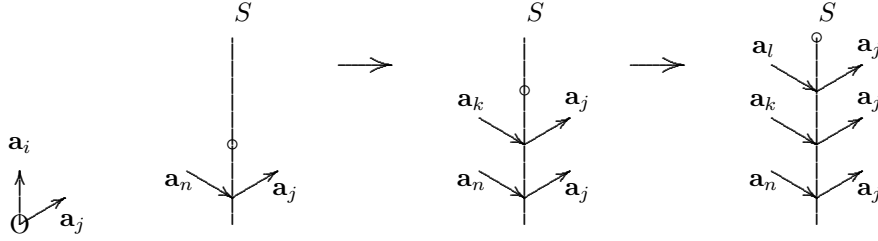


**Figure 12.** The case in Figure 11(b). If  $Q$  is a plane coplanar with  $\{\mathbf{d}_j, \mathbf{d}_n\}$  then  $S$  is the line  $S = Q \cap P_r$ . If one moves along  $S$  in the vertical sense here, then eventually one must encounter an open vertex  $\circ$ . In this case the moves in Figure 11(b) can be systematically performed on each of the isolated vertices along  $S$ , starting at the top. This will translate all the edges on the left of  $S$  through the plane  $P_r$  towards the right in the  $\mathbf{d}_j$  direction.

Since the polygon is finite we eventually must find a vacant vertex — as shown in the rightmost part of Figure 12. The edge (depicted as  $\mathbf{d}_l$ ) can then be translated in the  $\mathbf{d}_j$  direction. This (effectively) moves the vacant vertex back along  $P_r$  and so one recursively apply this construction until we finally move the desired edge,  $\mathbf{d}_n$ , in the  $\mathbf{d}_j$  direction, using the construction in Figure 11(b).

The stretching of the polygon in a new plane,  $Q_r$ , in the transverse (to  $Q_r$ ) direction  $\mathbf{d}_j$ , proceeds by first finding the right most line in the projection, and lifting it to the plane  $P_r$  (parallel to  $Q_r$ ). The polygon is then stretched one step in the  $\mathbf{d}_j$  direction in  $P_r$ . Then  $P_r$  is moved closer to  $Q_r$  one step in the  $-\mathbf{d}_j$  direction and the polygon is stretched recursively until it is finally  $P_r$  is coincident with  $Q_r$  in which case the polygon is stretched one step in the  $\mathbf{d}_j$  direction on one side of  $Q_r$ .

The effect of this construction is to cut the polygon along the plane  $Q_r$  into a left part and right part. The right part is then translated in the  $\mathbf{d}_j$  direction and the two parts are reconnected by inserting edges in the  $\mathbf{d}_j$  direction.

In topological terms this construction is an (orientation preserving) ambient isotopy of three space, and it does not change the knot type of the polygon. We say that the polygon  $\omega$  was *stretched* in the  $\mathbf{d}_j$  direction transverse to the plane  $Q_r$ .

This construction proves the following lemma:

**Lemma 7** *Let  $\omega$  be any FCC lattice polygon and let  $Q_r$  be a lattice plane intersecting  $\omega$ . Then  $\omega$  can be stretched, using the FCC elementary move, in  $Q_r$  in the  $\mathbf{d}_j$  direction if  $\mathbf{d}_j$  is transverse to  $Q_r$ .*

*Proof:* Since  $Q_r$  is a lattice plane, determine a plane  $A$  transverse to it which intersects the FCC in a triangular lattice. Orient the projected polygon as above, and then use the elementary moves to stretch the polygon in  $Q_r$  in the desired direction as described by the construction above.  $\diamond$

#### 4.3. Contact free FCC lattice polygons

As was the case for the BCC lattice, care must be taken to ensure that different pieces of the polygon do not come too close together while we try to sweep it onto a simple cubic sublattice. Thus we define *contacts* on the FCC lattice in the same way we did on the BCC lattice; two non-adjacent vertices  $\mathbf{u}$  and  $\mathbf{v}$  in a polygon  $\omega$  form a *contact* if  $\mathbf{u} - \mathbf{v} = \mathbf{d}_j$  for some  $j$ . That is, these vertices are a distance  $\sqrt{2}$  apart in the FCC.

A polygon  $\omega$  is *contact free* if it has no contacts. We next show that we can use the FCC elementary move to transform any polygon into a contact free polygon.

Lemma 7 shows that any given polyon can be stretched in the  $\mathbf{d}_j$  direction transverse to a plane  $Q_r$  (which intersects the FCC lattice in a triangular sublattice).

If a polygon is stretched in every transverse direction in every lattice plane  $Q$  which intersects it in a triangular lattice, then the effect is to double the length of every edge of the polygon. That is, each edge gets replaced by two edges. This is a *subdivision* of the polygon  $\omega$ . One may repeat this stretching several times to stretch each edge any number of times.

If polygon has a contact in the  $\mathbf{d}_j$  direction, then it is removed if the polygon is subdivided once since all distances between vertices in the polygon is increased by at least a factor of 2 in a subdivision of the polygon. In addition, a contact in the  $\mathbf{d}_j$  direction cannot be created if the polygon is stretched in the  $\mathbf{d}_i$  direction, since the relative orientations of vertices and edges in the  $\mathbf{d}_j$  direction is maintained if the stretching is in the  $\mathbf{d}_i$  direction.

Thus, one may remove all contacts from a polygon by stretching or by subdivision. This leaves a contact free polygon, and we proved the following lemma.

**Lemma 8** *By subdividing an FCC polygon, it is possible to transform it into a contact free polygon, using the FCC elementary move.*

*Proof:* Consider a (non-orthogonal) projection  $P\omega$  of an FCC polygon  $\omega$  into a lattice plane  $A$  along a lattice direction transverse to  $A$ , where  $A$  intersects the FCC in a triangular lattice  $\mathbb{L}_t$  with basis vectors (say)  $\mathbf{d}_i$ ,  $\mathbf{d}_j$  and  $\mathbf{d}_k$ .

The projection  $P\omega$  cuts the plane  $A$  into one infinite face and a set of finite faces (or areas). Each finite face has an area measured in units of the elementary triangle in the triangular lattice.

Since  $\mathbf{d}_i$  is a basis vector of the sublattice  $\mathbb{L}_t$ , a subdivision of  $\omega$  in the  $\mathbf{d}_i$  direction increases the area of each finite face in the projection in the plane  $A$  by at least one unit elementary triangle. This is similarly true when subdividing in the  $\mathbf{d}_j$  and  $\mathbf{d}_k$  directions.

Contacts in the FCC polygon which are oriented in the  $\mathbf{d}_i$ ,  $\mathbf{d}_j$  and  $\mathbf{d}_k$  directions will project in the plane  $A$  as edges in  $\mathbb{L}_t$ . A subdivision in the direction of a given contact will remove it from the projection, and thus also from the polygon itself.

If subdivisions in the  $\mathbf{d}_i$  direction removed all contacts in this direction, then subsequent subdivision in other directions will not create contacts in the  $\mathbf{d}_i$  direction (since this would require the translation of parts of the polygon in the  $\mathbf{d}_i$  direction, and this cannot occur).

Hence, by using subdivisions of  $\omega$  in each of the six independent directions of the FCC lattice, all contacts are removed from the polygon, and it becomes contact free. This completes the proof.  $\diamond$

#### 4.4. Pushing contact free FCC polygons into a simple cubic sublattice

Let  $\mathbb{L}$  be that sublattice of the FCC with basis vectors  $\{\mathbf{d}_1, \mathbf{d}_3, \mathbf{d}_5, \mathbf{d}_7, \mathbf{d}_9, \mathbf{d}_{11}\}$ . Then  $\mathbb{L}$  is ambient isotopic to the simple cubic lattice.

If  $\omega$  is a polygon in  $\mathbb{L}$ , then the (simple cubic lattice) BFACF move (see Figure 1) can be performed on  $\omega$  in  $\mathbb{L}$  by composing two FCC elementary moves in order to execute each single BFACF move. For example, the positive BFACF move  $\mathbf{d}_1 \rightarrow \mathbf{d}_3\mathbf{d}_1\mathbf{d}_9$  can be performed in the two step sequence  $\mathbf{d}_1 \rightarrow \mathbf{d}_3\mathbf{d}_6 \rightarrow \mathbf{d}_3\mathbf{d}_1\mathbf{d}_9$ .

In other words, the irreducibility properties of FCC lattice polygons in the sublattice  $\mathbb{L}$  is determined by the irreducibility properties of the simple cubic lattice BFACF moves, and by Theorem 1. We shall use these facts to complete the proof that the irreducibility classes of the FCC elementary move on unrooted FCC lattice polygons coincide with the knot types of the polygons as piecewise linear embeddings in three space.

The strategy is as follows: If  $\omega$  is an FCC lattice polygon, then it will be moved to a polygon in the sublattice  $\mathbb{L}$ , from where it will be put in standard position  $\lambda$  given its knot-type  $K$ . Since the composition of all the FCC elementary moves is a continuous piecewise linear orientation preserving isotopy of three space, we know that the polygon  $\lambda$  in standard position has the same knot type  $K$ , and moreover, that every polygon can be moved to  $\lambda$  using a finite number of FCC elementary moves.

It only remains to prove that every FCC lattice polygon can be moved to a polygon in  $\mathbb{L}$ .

**Lemma 9** *By using the FCC elementary move, any FCC lattice polygon  $\omega$  can be swept into a sublattice  $\mathbb{L}$  of the FCC, where  $\mathbb{L}$  is ambient isotopic to the simple cubic lattice.*

*Proof:* Since every polygon can be made contact free, it is enough to assume that  $\omega$  is contact free. We next prove that every such contact free polygon can be moved into the lattice  $\mathbb{L}$ .

If  $\omega$  is embedded in  $\mathbb{L}$ , then we are done.

Otherwise,  $\omega$  has some edges in directions from the set  $\{\mathbf{d}_2, \mathbf{d}_4, \mathbf{d}_6, \mathbf{d}_8, \mathbf{d}_{10}, \mathbf{d}_{12}\}$ . Since  $\omega$  is contact free, the FCC elementary move can be performed on each of each of the edges in  $\omega$  without creating self-intersections.

Proceed along the polygon and remove edges in the  $\mathbf{d}_{10}$ ,  $\mathbf{d}_2$ ,  $\mathbf{d}_4$ ,  $\mathbf{d}_6$ ,  $\mathbf{d}_8$ ,  $\mathbf{d}_{10}$  and  $\mathbf{d}_{12}$  directions systematically by replacing them as follows:

$$\begin{aligned} \mathbf{d}_2 &\rightarrow \mathbf{d}_3\mathbf{d}_{11}, & \mathbf{d}_4 &\rightarrow \mathbf{d}_1\mathbf{d}_{11}, & \mathbf{d}_6 &\rightarrow \mathbf{d}_9\mathbf{d}_5, \\ \mathbf{d}_8 &\rightarrow \mathbf{d}_9\mathbf{d}_5, & \mathbf{d}_{10} &\rightarrow \mathbf{d}_7\mathbf{d}_5, & \mathbf{d}_{12} &\rightarrow \mathbf{d}_3\mathbf{d}_7. \end{aligned}$$

If during this process a contact is created, then the polygon is again swept in the  $\{\mathbf{d}_1, \mathbf{d}_3, \mathbf{d}_5\}$  directions. Each contact will have a non-zero projection along at least one of these directions, and will then be removed without inserting any new edges in any directions apart from those in the simple cubic sublattice  $\mathbb{L}$ . Finally, these elementary moves will move  $\omega$  into the sublattice  $\mathbb{L}$ .  $\diamond$

A direct corollary of this lemma is

**Theorem 10** *The irreducibility classes of the FCC elementary move, applied to unrooted polygons in the FCC, coincides with the knot types of the polygons as piecewise linear embeddings in  $\mathbb{R}^3$ .*

*Proof:* Observe that since  $\mathbb{L}$  is a sublattice of the FCC which is isotopic to the simple cubic lattice, the irreducibility classes of the FCC elementary move applied to unrooted polygons in  $C$  coincides with the knot types of the polygons as piecewise linear embeddings in  $\mathbb{R}^3$ . This follows directly from the observation above that all BFACF moves on a polygon in  $\mathbb{L}$  can be induced by using the FCC elementary move, and from Theorem 1 or Theorem 3.11 in reference [16].

By Lemma 9 any unrooted polygon in the FCC can be (reversibly) swept into the sublattice  $\mathbb{L}$  using the FCC elementary move.

Standard BFACF elementary moves in the sublattice  $\mathbb{L}$  can be performed by combining FCC elementary moves. For example, the positive move  $\mathbf{d}_1 \rightarrow \mathbf{d}_3\mathbf{d}_1\mathbf{d}_9$  in  $\mathbb{L}$  is a BFACF move, and it is performed in two steps in the FCC by  $\mathbf{d}_1 \rightarrow \mathbf{d}_3\mathbf{d}_{12} \rightarrow \mathbf{d}_3\mathbf{d}_1\mathbf{d}_9$ , since  $\mathbf{d}_1 = \mathbf{d}_3 + \mathbf{d}_{12}$  and  $\mathbf{d}_{12} = \mathbf{d}_1 + \mathbf{d}_9$ . The other cases, and neutral and negative SC BFACF moves can similarly be checked.

Hence, since the standard SC BFACF moves in Figure 1 can be performed on the polygon in  $\mathbb{L}$ , using composite FCC elementary moves, the theorem follows immediately.  $\diamond$

## 5. Conclusions and implementation

In this paper we have shown that the BFACF elementary moves on simple cubic lattice polygons can be generalised to similar moves on the BCC and FCC lattices. For the BCC lattice, we propose a set of four elementary moves (two are neutral, and two are positive/negative), while on the FCC lattice we propose a single (reversible) elementary move (of type positive/negative).

We proved that, on the BCC and FCC lattices, these moves are suitable to give irreducibility classes of unrooted polygons that coincide with the knot types of the polygons. This is, we have generalised Theorem 3.11 in reference [16] to both the FCC and BCC lattices. For the BCC lattices, our method of proof relied on all four proposed elementary moves and so we know that these moves are sufficient. It is not clear that any of these are necessary, or that a smaller set of similarly defined elementary moves may be sufficient.

Using the proposed moves we have implemented the GAS algorithm [14] to sample knotted polygons on both the FCC and BCC lattices. We give some results in Table 1 and further numerical results will be published elsewhere.

### 5.1. The GAS implementation of the BCC and FCC elementary moves

In the GAS implementation [14] of the algorithm, lattice polygons of (fixed) knot type  $K$  are sampled along a Markov Chain by executing the elementary (or atmospheric) moves on the polygons. Let  $\phi = \langle \phi_n \rangle = \langle \phi_0, \phi_1, \phi_2, \dots \rangle$  be a realisation of a sequence started in the initial state  $\phi_0$ , which is a polygon of length  $\ell(\phi_0)$  and of knot type  $K$ .

A state  $\phi_{n+1}$  from  $\phi_n$  is generated as follows: Let  $A_+(\phi_n)$  be the set of all positive atmospheric or elementary moves on the polygon  $\phi_n$ , and similarly,  $A_0(\phi_n)$  and  $A_-(\phi_n)$  the set of all neutral and negative atmospheric moves on  $\phi_n$ . These are the positive, neutral and negative *atmospheres* of  $\phi_n$ .

Define the sizes of the of the positive, neutral and negative atmospheres of  $\phi_n$  by  $a_+(\phi_n)$ ,  $a_0(\phi_n)$  and  $a_-(\phi_n)$ . If  $\ell(\phi_n) = N$ , then each of these statistics has a mean value denoted by  $\langle a_+ \rangle_N$ ,  $\langle a_0 \rangle_N$  and  $\langle a_- \rangle_N$ .

Next, define a set of parameters of the GAS algorithm by

$$\beta_N = \frac{\langle a_- \rangle_N}{\langle a_+ \rangle_N}. \quad (2)$$

With these definitions, one may now determine  $\phi_{n+1}$ .

The state  $\phi_{n+1}$  is obtained from  $\phi_n$  by selecting with probability  $P_+$  a positive atmospheric move, with probability  $P_0$  a neutral atmospheric move, and with probability  $P_-$  a negative atmospheric move, and executing it on  $\phi_n$  to obtain  $\phi_{n+1}$ . In each case, once a determination is made to execute a move, the move is selected

uniformly from amongst the available moves in each of the sets  $A_+(\phi_n)$ ,  $A_0(\phi)$  and  $A_-(\phi_n)$ .

The probabilities  $P_+$ ,  $P_0$  and  $P_-$  are given by

$$\begin{aligned} P_+ &= \frac{\beta_N a_+(\phi_n)}{a_-(\phi_n) + a_0(\phi_n) + \beta_N a_+(\phi_n)}; \\ P_0 &= \frac{a_0(\phi_n)}{a_-(\phi_n) + a_0(\phi_n) + \beta_N a_+(\phi_n)}; \\ P_- &= \frac{a_1(\phi_n)}{a_-(\phi_n) + a_0(\phi_n) + \beta_N a_+(\phi_n)}, \end{aligned}$$

where  $N = \ell(\phi_n)$  is the length of the polygon  $\phi_n$ , and  $\beta_N$  is estimated by updating it recursively in the simulation.

This implementation give a sequence  $\phi = \langle \phi \rangle_M$  of  $M + 1$  states sampled from polygons of knot type  $K$ . The analysis of the data sequence depends on a weight  $W(\phi)$  of the sequence, which is defined as follows: Define  $\sigma(n, n + 1) = -1$  if  $\phi_n \rightarrow \phi_{n+1}$  via a positive atmospheric move, and  $\sigma(n, n + 1) = 1$  if  $\phi_n \rightarrow \phi_{n+1}$  via a negative atmospheric move. Then the weight of the sequence  $\phi$  is given by

$$W(\phi) = \left[ \frac{a_-(\phi_0) + a_0(\phi_0) + \beta_{\ell(\phi_0)} a_+(\phi_0)}{a_-(\phi_L) + a_0(\phi_L) + \beta_{\ell(\phi_L)} a_+(\phi_L)} \right] \prod_{n=0}^{|\phi|-1} \beta_{\ell(\phi_n)}^{\sigma(n, n+1)}, \quad (3)$$

where  $\ell(\phi_n)$  is the length (number of edges) in polygon  $\phi_n$ , and where  $L = |\phi|$  is the length (number of states) in the sequence  $\phi$ .

The expected value of the weight of sequences ending in states of length  $N$  is  $\langle W(\phi) \rangle_N$ , and the basic GAS theorem states that

$$\frac{\sum_{|\tau|=N} \langle W(\tau) \rangle_N}{\sum_{|\rho|=M} \langle W(\rho) \rangle_M} = \frac{p_N(K)}{p_M(K)}, \quad (4)$$

where  $\tau$  are all possible sequences of states ending in a state of length  $|\tau| = N$ , and  $\rho$  are all the possible sequences of states ending in a state of length  $|\rho| = M$ .

In this implementation, the FCC and BCC elementary moves described in this paper will give an approximate enumeration algorithm, and estimates of the number of polygons of knot type  $K$  and length  $n$ ,  $p_n(K)$ , can be obtained. This approach produced the data in table 1.

## 5.2. The BFACF-style implementation of the BCC and FCC elementary moves

The GAS algorithm is by no means a standard simulation method (though the authors hope that it might become more popular), and so we finish the paper by discussing how the proposed moves may be implemented in a BFACF-style algorithm, as implemented in reference [2, 5]; further implementations can be found in references [6, 18].

In general the BFACF algorithm is applied to either a self-avoiding walk or self-avoiding polygons and so we will discuss the implementation of the BCC and FCC moves to sample either walks or polygons. Since these moves do not translate the endpoints of a self-avoiding walk, assume that the walk is rooted at its endpoints. The simple cubic lattice moves are not irreducible on the state space  $S_{0x}$  of walks with fixed endpoints 0 (the origin) and a lattice site  $x$  [8, 16] unless those endpoints are a distance of at least 2 apart (for details, see reference [8]). We believe that a similar result will hold for the BCC and FCC moves we have proposed, but we have not yet investigated this.

Let  $\omega_n$  be the current walk or polygon (or “state”) of length  $|\omega_n|$  edges. Choose an edge  $s$  from  $\omega_n$  with uniform probability. Enumerate the possible elementary moves on  $s$ ; in the BCC lattice there are 12 possible moves while in the FCC there are 4 possible moves. At most one these elementary moves is a negative atmospheric move (will shorten the polygon or walk), while the remaining moves are positive or neutral.

Choose one of the possible moves so that a particular positive move is done with probability  $P_+$ , a particular negative move is carried out with probability  $P_-$  and a particular neutral elementary move is performed with probability  $P_0$ . This produces a state  $\omega'_n$ . If this state is self-avoiding then we accept it and set  $\omega_{n+1} = \omega'_n$  and otherwise we reject it and set  $\omega_{n+1} = \omega_n$ . It remains to specify the probabilities  $P_+$ ,  $P_-$  and  $P_0$ , and hence a probability is attached to each of these moves. This must be done differently on each lattice.

Consider a polygon or walk in the BCC lattice and a given edge  $s$ . The possible moves we can perform on  $s$  depend on the conformation of the of  $s$  and its predecessor and successor edges. In particular, the moves on a given edge are in one the following classes:

- All the possible moves on the edge  $s$  are positive elementary moves increasing the length of the walk or polygon; this gives 12 positive elementary moves on  $s$ .
- The possible elementary moves include 11 positive and 1 neutral move; denote this as  $(11, 1, 0)$ .
- The possible elementary moves include 10 positive and 2 neutral moves; denoted by  $(10, 2, 0)$ .
- The possible elementary moves include 9 positive, 2 neutral and 1 negative moves; denoted by  $(9, 2, 1)$ .
- Similarly, the following combinations are possible  $(9, 3, 0)$ ,  $(8, 4, 0)$ ,  $(7, 4, 1)$  and  $(6, 6, 0)$ .

In addition, one has the Boltzmann type relation  $P_+ = e^{-2\beta}P_-$  relating the probability of making a positive elementary move, to that of making a negative elementary move. The cases above sets up a set of bounds on the different probabilities:

$$\begin{array}{ll} 12P_+ & \leq 1; & 11P_+ + P_0 & \leq 1; \\ 10P_+ + 2P_0 & \leq 1; & 9P_+ + 3P_0 & \leq 1; \\ 9P_+ + 2P_0 + P_- & \leq 1; & 8P_+ + 4P_0 & \leq 1; \\ 7P_+ + 4P_0 + P_- & \leq 1; & 6P_+ + 6P_0 & \leq 1. \end{array}$$

We need to maximise the value of  $P_+$  while satisfying these bounds . Since  $\beta > 0$  and  $P_+ = e^{-2\beta}P_-$ , it follows that  $P_+ \leq P_-$ . If we additionally assume that  $P_+ \leq P_0 \leq P_-$ , then the first six inequalities are redundant and one can simply study the last two (that is, the bottom row). Maximising then gives

$$P_+ = \frac{e^{-2\beta}}{3(1 + 3e^{-2\beta})}, \quad P_0 = \frac{1 + e^{-2\beta}}{6(1 + 3e^{-2\beta})}, \quad P_- = \frac{1}{3(1 + 3e^{-2\beta})}. \quad (5)$$

Note that  $P_0 = \frac{1}{2}(P_+ + P_-)$ .

The situation is simpler on the FCC lattice due to the simplicity of the elementary move. When an edge  $s$  is selected from the polygon there are only two possibilities:

- the four possible moves on the edge  $s$  are positive elementary moves
- three of the possible elementary moves are positive and one is a negative elementary move.



This gives the following set of inequalities for the probabilities  $P_+$ , and  $P_-$ :

$$4P_+ \leq 1; \quad 3P_+ + P_- \leq 1.$$

Since there are no neutral moves in the FCC algorithm we do not require  $P_0$  (or we can simply set  $P_0 = 0$ ). Again we have a Boltzmann factor relating the probabilities, namely  $P_+ = e^{-\beta}P_-$  with  $\beta > 0$ . Since  $P_+ \leq P_-$  the first of these equations is redundant, and the second gives

$$P_+ = \frac{e^{-\beta}}{1 + 3e^{-2\beta}}, \quad P_- = \frac{1}{1 + 3e^{-\beta}}. \quad (6)$$

With the above choices of  $\{P_+, P_0, P_-\}$  on either the BCC or FCC lattices, the algorithm for polygons runs as described below. The algorithm for walks is identical after the initialisation step.

1. Initialise the algorithm by choosing the first polygon,  $\omega_0$ , to be a polygon of given length and desired knot type  $K$ . Define the parameter  $\beta$ . The length of this initial polygon is not crucial except that it must be sufficiently long to embed a knot of type  $K$ .
2. Let  $\omega_n$  be the current polygon of length  $|\omega_n|$  edges. With uniform probability,  $1/|\omega_n|$ , choose an edge  $s$  in  $\omega_n$ . Enumerate all possible elementary moves which can be performed on that edge.
3. With probability  $P_+$  perform a (particular) positive atmospheric move, uniformly selected from amongst all the possible positive moves. Similarly, with respectively probabilities  $P_0$  or  $P_-$ , perform a particular neutral or negative move. If the sum of these probabilities is less than 1, then the remaining default move is to leave the polygon unchanged.
4. Step 3 induces a proposed polygon  $\omega'_n$ . If the proposed polygon is not self-avoiding, or if (by default) no elementary move occurred, then  $\omega'_n = \omega_n$ .
5. Put  $\omega_{n+1} = \omega'_n$  to find the next state, and continue at step 2 above.

In this implementation the transition probability of obtaining a polygon  $\tau$  from a given polygon  $\omega$ ,  $P_{\omega \rightarrow \tau}$ , is given by

$$P_{\omega \rightarrow \tau} = \begin{cases} [P_+ / |\omega|], & \text{if the elementary move is positive;} \\ [P_- / |\omega|], & \text{if the elementary move is negative;} \\ [P_0 / |\omega|], & \text{if the elementary move is neutral,} \end{cases} \quad (7)$$

since the edge  $S$  is selected with a priori probability  $1/|\omega|$  before the elementary move is performed. These transition probabilities satisfy the condition of detailed balance between states  $\omega$  and  $\tau$  given by

$$|\omega| P_{\omega \rightarrow \tau} = |\tau| P_{\tau \rightarrow \omega}, \quad (8)$$

with the result that, in the BFACF-style implementation, the algorithm will sample asymptotically from the distribution

$$P_\beta(\omega) = \frac{|\omega| e^{\beta|\omega|}}{\sum_\tau |\tau| e^{\beta|\tau|}} = \frac{|\omega| e^{\beta|\omega|}}{\sum_n n p_n(K) e^{\beta n}}, \quad (9)$$

where  $p_n(K)$  is the number of polygons of length  $n$  edges and knot type  $K$ , since the algorithm is ergodic on the class of unrooted polygons with fixed knot type  $K$ . This

is not the canonical Boltzmann distribution over the state space of unrooted polygons with knot type  $K$  given by

$$P'_\beta(\omega) = \frac{e^{\beta|\omega|}}{\sum_\tau |\tau| e^{\beta|\tau|}} = \frac{e^{\beta|\omega|}}{\sum_n n p_n(K) e^{\beta n}}. \quad (10)$$

Note that denominator is finite when  $\beta < -\log \mu_K$  where  $\mu_K$  is the growth constant of polygons of given knot type defined by

$$\limsup_{n \rightarrow \infty} [p_n(K)]^{1/n} = \mu_K. \quad (11)$$

This limit is known to exist for the unknot, but its existence for other knot types is a long standing open problem.

### 5.3. Metropolis-style implementation of BCC and FCC elementary moves

A simpler implementation of the BCC and FCC elementary moves uses the Metropolis algorithm. In this case steps **2** and **3** above are modified as follows: Choose an edge  $s$  with uniform probability  $1/|\omega_n|$  in the current polygon, and select (uniformly) one of the 12 possible elementary plaquettes on the edge in the BCC lattice, or one of 4 possible elementary plaquettes on it in the FCC lattice. Then choose one of the elementary plaquettes uniformly and attempt the elementary move it defines. If the resulting object is self-avoiding polygon  $\omega'_n$  of length  $|\omega'_n|$  edges, then accept it with probability  $\min\{1, e^{\beta(|\omega'_n| - |\omega_n|)}\}$  as the next state  $\omega_{n+1}$ .

Otherwise, put  $\omega_{n+1} = \omega_n$ . In this implementation one can show that the condition of detailed balance is given by equation (8), and if  $\beta < -\log \mu_K$ , the algorithm samples asymptotically from the distribution  $P_\beta(s)$  in equation (9).

## Acknowledgments

The authors acknowledge funding in the form of Discovery Grants from NSERC (Canada).

## Bibliography

- [1] Aragão de Carvalho C and Caracciolo S 1983 *A New Monte Carlo Approach to the Critical Properties of Self-Avoiding Random Walks*. Phys Rev **B27** 1635-1645
- [2] Aragão de Carvalho C, Caracciolo S and Fröhlich J 1983 *Polymers and  $g|\phi|^4$ -theory in Four Dimensions*. Nucl Phys **B215** [FS7] 209-248
- [3] Baiesi M, Orlandini E and Stella A L 2007 *Ranking Knots of Random, Globular Polymer Rings*. Phys Rev Lett **99** 058301-5
- [4] Baiesi M, Orlandini E and Whittington S G 2009 *Interplay Between Writhe and Knotting for Swollen and Compact Polymers*. J Chem Phys **131** 154902-11
- [5] Berg B and Foester D 1981 *Random Paths and Random Surfaces on a Digital Computer*. Phys Lett **106B** 323-326
- [6] Brak R and Nidras P P 1997 *New Monte Carlo Algorithm for Interacting Self-Avoiding Walks*. J Phys A: Math Gen **30** 1457-1469
- [7] Downey J P, Crabb C C and Kovac J 1986 *Dynamics of a Face-Centered Cubic Lattice Model for Polymer Chains*. Macromol **19** 2202-2206
- [8] Janse van Rensburg E J 1992 *Ergodicity of the BFACF Algorithm in Three Dimensions*. J Phys A: Math Gen **25** 1031-1042
- [9] Janse van Rensburg E J 2008 *Thoughts on Lattice Knot Statistics*. J Math Chem **45**(1) 7-38 (Commemorative issue in honour of S Whittington and R Kapral)

- [10] Janse van Rensburg E J 2009 *Monte Carlo Methods for Lattice Polygons*. In *Polygons, Polyominoes and Polyhedra* Ed A J Guttmann (Canopus Publishing Ltd).
- [11] Janse van Rensburg E J, Orlandini E, Summers D W, Tesi M C and Whittington S G 1996 *The Writhe of Knots in the Cubic Lattice*. *J Knot Theo Ram* **6** 31-44
- [12] Janse van Rensburg E J and Promislow S D 1995 *Minimal Knots in the Cubic Lattice*. *J Knot Theo Ram* **4** 115-130
- [13] Janse van Rensburg E J and Rechnitzer A 2008 *Atmospheres of Polygons and Knotted Polygons*. *J Phys A: Math Theo* **41** 105002-25
- [14] Janse van Rensburg E J and Rechnitzer A 2009 *Generalised Atmospheric Sampling of Self-Avoiding Walks*. *J Phys A: Math Theo* **42** 335001-30
- [15] Janse van Rensburg E J and Rechnitzer A 2010 *Generalised Atmospheric Sampling of Knotted Polygons*. *J Knot Theo Ram* (to appear)
- [16] Janse van Rensburg E J and Whittington S G 1991 *The BFACF Algorithm and Knotted Polygons*. *J Phys A: Math Gen* **24** 5553-5567
- [17] Metropolis N, Rosenbluth A W, Rosenbluth M N, Teller A H and Teller E 1953 *Equation of State Calculations by Fast Computing Machines*. *J Chem Phys* **23** 1087-1092
- [18] Orlandini E, Janse van Rensburg E J and Whittington S G 1996 *A Monte Carlo Algorithm for Lattice Ribbons*. *J Stat Phys* **82** 1159-1198
- [19] Orlandini E, Janse van Rensburg E J and Whittington S G 1996 *A Monte Carlo Algorithm for Lattice Ribbons*. *J Stat Phys* **82** 1159-1198
- [20] Orlandini E, Tesi M C, Janse van Rensburg E J and Whittington S G 1998 *Asymptotics of Knotted Lattice Polygons*. *J Phys A: Math Gen* **31** 5953-5967
- [21] Quake S 1994 *Topological Effects of Knots in Polymers*. *Phys Rev Lett* **73** 3317-3320
- [22] Rechnitzer A and Janse van Rensburg E J 2008 *Generalised Atmospheric Rosenbluth Methods (GARM)*. *J Phys A: Math Theo* **41** 442002-442010
- [23] Rosenbluth M N and Rosenbluth A W 1955 *Monte Carlo Calculation of the Average Extension of Molecular Chains*. *J Chem Phys* **23** 356-359
- [24] Scharein R, Ishihara K, Arsuaga J, Diao Y, Shimokawa K and Vazquez M 2009 *Bounds for Minimal Step Number of Knots in the Simple Cubic Lattice*. *J Phys A: Math Theo* **42** 475006-30
- [25] Uberti R, Janse van Rensburg E J, Orlandini E, Tesi M C and Whittington S G 1996 *Minimal Links in the Cubic Lattice*. *Topology and Geometry in Polymer Science*, Ed. S.G. Whittington, D.W. Sumners and T. Lodge. Proc 1995-1996 IMA, Workshop 8, June 10-16 1996